ORIGINAL RESEARCH

The Study of Endothelial-Mesenchymal Transition in an Atrial Fibrillation Rat Model

Wenhui Wang, MD; Xinming Li, MD; Zhongping Ning, MS

ABSTRACT

Background • Activated fibroblasts are reported partly of endothelial origin, derived through endothelial-mesenchymal transition (EndMT). Few studies have investigated EndMT in atrial fibrillation (AF), which may have a potential effect on cardiac fibrosis.

Objective • To investigate whether EndMT occurs in an animal model of AF.

Methods • A total of 80 Sprague–Dawley rats (8 weeks, male, 200-250 g) were randomly divided into two groups: the control group and the AF group (n = 40 in each group). Rats in the AF group received a daily intravenous injection of acetylcholine-calcium chloride for seven days to establish an AF model, and rats in the control rats were injected with saline in the same way. At different time points (Day 3, Day 5, Day 7, Day 9, Day 11, Day 13, Day 15, and Day 17), we observed changes in EndMT-related indexes (CD31, VE-cadherin, FSP-1, TGF-β1 and collagen) and HIF-1α in the rat atria of two groups, as well as immunofluorescence co-expression of CD31/FSP-1 and VE-cadherin/FSP-1 in the endocardial endocardium of the atria.

Results • In the AF group, atrial EndMT was observed and enhanced with time. Compared with the control group, the levels of CD31 and VE-cadherin in the AF group decreased, while mesenchymal marker (FSP-1) and EndMT inducer (TGF-β1) were dynamically increased after Day 3. The co-expression of CD31/FSP-1 and VE-cadherin/FSP-1 was observed from Day 3 to the end of observation time Day 17 by immunofluorescence in AF rat hearts, indicating the existence of EndMT. In addition, the level of HIF-1α in the hearts of AF rats was increased.

Conclusion • As far as we know, this is the first study to explore the dynamic process of EndMT in an AF rat model. The presence of EndMT was verified in the atria of the AF rat model, and Day 7-Day 17 was the best observation time point for the model. This may lead to a better understanding of the pathological changes and mechanisms in AF with a short modeling cycle. (*Altern Ther Health Med.* 2024;30(1):179-185).

Wenhui Wang, MD; Department of Cardiology, Shanghai East Hospital, School of Medicine, Tongji University, Shanghai, China; **Xinming Li, MD; Zhongping Ning, MS;** Department of Cardiology, Shanghai University of Medicine & Health Sciences Affiliated Zhoupu Hospital, Shanghai, China.

Corresponding author: Xinming Li, MD
E-mail: xinming06@163.com
Corresponding author: Zhongping Ning, MS
E-mail: ningzhongping88@126.com

INTRODUCTION

Atrial fibrillation (AF) is a common cardiovascular disorder that causes major disease, morbidity, and mortality.[1] Atrial fibrosis is a key factor linking AF-related pathogenesis.[2] Researchers worldwide are exploring the molecular mechanism of atrial fibrosis in AF from multiple aspects that may lead to the development of more effective targeted interventions.

Activated fibroblasts are partly of endothelial origin, derived through endothelial-mesenchymal transition (EndMT).[3] During EndMT, endothelial cells (ECs) deform under the stimulation of shear stress, proinflammatory factors, hypoxia, and other factors, changing their phenotypes and eventually participating in the fibrotic process.[4] These phenotypes include the decrease of specific endothelial markers such as cluster of differentiation 31 (CD31) and vascular endothelial cadherin (VE-cadherin) and the increase of mesenchymal markers such as alpha-smooth muscle actin and fibroblast-specific protein-1 (FSP-1).[4]

The EndMT has been reported in several animal models, including aortic coarctation or angiotensin II-induced cardiomyopathy, diabetic cardiomyopathy, myocardial infarction, and cardiac insufficiency caused by asynchronous ventricular pacing.[5-9] However, the contribution of EndMT in cardiac fibrosis remains controversial.[10] In 2017, Kato et al. first proposed that EndMT occurred in the atria of patients

with AF, and the level of mesenchymal markers was positively correlated with the degree of atrial structural remodeling.[11] The downside was that the result had not been compared to normal hearts. To the best of our knowledge, there are still significant gaps in the area of the EndMT process in AF patients or animal models.

In this study, we established an acetylcholine (Ach)-calcium chloride ($CaCl_2$)-induced rat model of AF and investigated whether EndMT progressed in this animal model; if it existed, we evaluated the optimal time point for EndMT, providing a stable animal model for further study of atrial fibrosis in AF.

METHODS

Materials and Facilities

The primary antibodies hypoxia-inducible factor-1 alpha (HIF-1α) monoclonal antibody (66730-1-Ig), CD31 polyclonal antibody (28083-1-AP), FSP-1 polyclonal antibody (20886-1-AP), transforming growth factor-beta 1 (TGF-β1) polyclonal antibody (21898-1-AP), Collagen-I monoclonal antibody (67288-1-Ig), and anti-β-actin (AF0003) were obtained from Proteintech Group (Proteintech Group, Inc. Wuhan, Hubei, China), and anti-VE-cadherin was obtained from Abcam (ab231227, Abcam Shanghai Trading Co., Ltd., Shanghai, China). Horseradish peroxidase-labeled goat anti-rat IgG(H+L) antibody was obtained from Beyotime Bio (A0192; Beyotime Biotechnology, Shanghai, China). Primers for target genes (HIF-1α, CD31, VE-cadherin, FSP-1, TGF-β1) were synthesized by General Biological System (Anhui) Co., Ltd. (Chuzhou, Anhui, China), and Glyceraldehyde phosphate dehydrogenase (GAPDH) was used as a standardization control. The primer sequences are shown in Supplementary Table 1. The Ach-$CaCl_2$ mixture (Ach 60 μg/mL + $CaCl_2$ 10 mg/mL) was obtained from Shanghai McLean Biochemical Technology Co., Ltd. (Shanghai, China). Electrocardiogram (ECG) monitoring (UM8000EV) was obtained from Wuhan WeissBioTech Co., Ltd. (Wuhan, Hubei, China).

Animals and Treatment

The animal experiment protocol was approved by the Ethics Committee of Tongji University (Approval number: TJAA12522201) and is consistent with the National Institutes of Health Guide for the Care and Use of Laboratory Animals.[12] A total of 80 healthy Sprague–Dawley (SD) rats (8 weeks, male, 200-250 g) were obtained from Shanghai JieSiJie Laboratory Animal Co., Ltd. (Shanghai, China) and housed under the following conditions: 20-25°C, 20%-25% relative humidity, regular photoperiod, adequate food and water. After one week of adaptive feeding, the rats were randomly divided into two groups based on a computer-generated random order: the control group and the AF group (n = 40 in each group).

For rats in the AF group, an Ach-$CaCl_2$ mixture (Ach 60 μg/mL + $CaCl_2$ 10 mg/mL) was injected through the tail vein at a dose of 1 mL/kg, once a day for 7 consecutive days.[13]. The control group rats were injected with 1 mL/kg of 0.9% normal saline with the same method for seven days. ECG monitoring (UM8000EV) was used to monitor the ECG of each rat during the peri-experimental period. Rats were fixed after being anesthetized (sodium pentobarbital, 50 mg/kg, intraperitoneal injection). Afterward, five 25-gauge hypodermic needle electrodes were inserted subcutaneously into four limbs and the front chest of the rat in sequence (noting that the needle was not inserted too deeply or it might cause interference). The monitoring was continued for 10 min after the graph was stabilized. After that, the AF rats were injected with Ach-$CaCl_2$ slowly and uniformly, while the control group was injected with normal saline; the ECG monitoring was continued for 20 minutes, and the AF rhythm was marked.

At the time point of Day 3, Day 5, Day 7, Day 9, Day 11, Day 13, Day 15, and Day 17, five rats of the control group and the AF group were randomly selected respectively, anesthetized, and fixed. After monitoring and possible treatment, the rats were euthanized (cervical dislocation under deep anesthesia). The heart was isolated and fixed with 4% paraformaldehyde for 24 hours, and then 5 μm thick paraffin sections were prepared for subsequent experiments. Partial atrial fragments were immediately stored at -80°C; part of the atrial fragments was washed with DEPC water, followed by the addition of precooled TRIZOL reagent, and then the fragments were stored at -80°C.

Hematoxylin and eosin (HE) and Masson Staining

HE and Masson staining of prepared paraffin sections was done as previously reported.[13] The histological changes in the atria were observed under an optical microscope (CKX41, Olympus, Tokyo, Japan) at ×40, ×100, and ×200 magnifications. Collagen was stained blue while myocardial tissue was red in Masson staining.

Immunohistochemistry

After the pre-experiment, the optimal antibody concentration was diluted to 1:500. Negative and positive control slides were set up. The prepared paraffin sections were deparaffinized, washed with PBS, and then infiltrated with prewarmed blocking permeabilization solution (40 mL PBS+120 μL TritonX-100+400 μL 30% H_2O_2) for 30 min (protected from light) to reduce the activity of endogenous peroxidase. The slides were treated with 0.01 mol/L sodium citrate buffer at pH 6.0 for antigen retrieval, boiled under high pressure for 4 minutes, cooled to room temperature 2 times, washed with PBS 3 times, and then marked with an oil pen. Nonspecific binding sites were blocked with serum homologous to the secondary antibody for 30 minutes, and excess serum was aspirated. Sections were then incubated with anti-HIF-1α (1:400; 66730-1-Ig, Proteintech) overnight at 4°C. Subsequently, the rewarmed and PBS-washed sections were incubated with a secondary antibody (1:500; A0192, Beyotime Bio) at room temperature for 1 hour and stained with freshly prepared diaminobenzidine-H_2O_2 for 10 minutes. Finally, the sections were counterstained with hematoxylin (nuclei) and analyzed under the optical microscope. Brown granular material was positive for HIF-1α.

Immunofluorescence

After deparaffinization, antigen retrieval, and blocking as previously described, paraffin sections were incubated with the anti-FSP-1 (1:200; 20886-1-AP, Proteintech) overnight at 4°C, rewarmed, PBS-washed, and incubated (37°C, 4 h) with FITC-affinipure fluorescent secondary antibody (1:200; A0562, Beyotime Bio) diluted in PBS containing 2% BSA. Next, the sections were incubated with another primary antibody, anti-CD31 (1:200; 28083-1-AP, Proteintech) or anti-VE-cadherin (1:200; ab231227, Abcam), and Cy3-affinipure fluorescent secondary antibody (1:200; A0516, Beyotime Bio) following the previous procedure. Finally, the sections were mounted with an anti-quenching reagent and analyzed under the fluorescence microscope with laser (CKX41, Olympus, Tokyo, Japan). EndMT was characterized by co-expression of CD31/FSP-1 or VE-cadherin/FSP-1 in ECs.[14] Observers counted CD31+/VE-cadherin+ and FSP-1+ ECs in 5 different endocardial regions of each sample and calculated the proportion of FSP-1+ ECs. All counts were performed independently by 2 observers.

Western Blot

Atrial fragments of the heart tissues (approximately 15 mg) were cut from the stored rat hearts after thawing, minced, and homogenized in RIPA buffer (500 μL), and the supernatant was extracted. The protein concentration of the supernatant was measured with a BCA kit (Shanghai Beenbio Medical Technology Center, Shanghai, China) and diluted to 5 ug/μL with SDS. Then the protein samples were separated by the SDS-polyacrylamide gel electrophoresis as previously reported and analyzed in a BIO-RAD gel imager (United States).[15] The primary antibodies were as follows: anti-CD31 (125 kDa; 28083-1-AP, Proteintech), anti-VE-cadherin (87 kDa; ab231227, Abcam), anti-FSP-1 (41 kDa; 20886-1-AP, Proteintech), anti-HIF-1α (110 kDa; 66730-1-Ig, Proteintech), anti-TGF-β1 (44 kDa; 21898-1-AP, Proteintech), anti-collagen-I (139 kDa; 67288-1-Ig, Proteintech) and anti-β-actin (36 kDa; AF0003, Proteintech) as control bands. The results were repeated three times and analyzed by the Image-Pro Plus 6.0 program.

Quantitative reverse transcription-polymerase chain reaction (qRT-PCR)

The thawed heart tissues in TRIZOL were chopped and homogenized on ice, and total RNA was extracted. After reverse transcription, the cDNA template and primers were subjected to the following reaction conditions for 40 cycles (95°C, 2 min; 95°C, 15 sec; 60°C, 60 sec) using an ASA-9600 Real-time PCR System (Suzhou Baiyuan Gent Co., Ltd., Suzhou, Zhejiang, China). Triplicate results were analyzed using the $2^{-\Delta\Delta Ct}$ method, GAPDH as a normalization control.[16]

Statistical Analysis

The experiment was carried out in triplicate. Quantitative data that conformed to a normal distribution were expressed as the mean ± standard deviation. *t* test and factorial analysis of variance were used for comparisons between groups, considering $P < .05$ as statistically significant. Analyses were performed using SPSS (version 26.0) and GraphPad Prism 9 software.

Figure 1. Successful establishment of the AF rat model. a. Electrocardiogram of the control group rats after injection. b. Electrocardiogram of the AFgroup rats after injection.

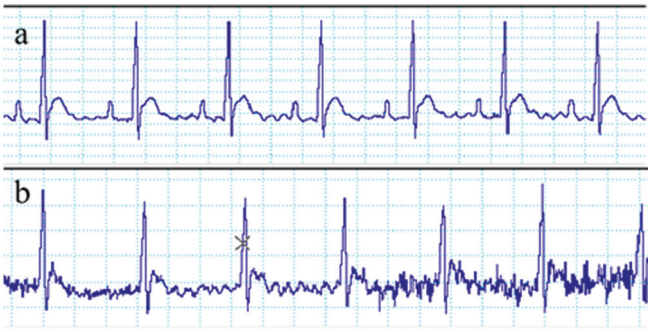

Figure 2. Histopathological changes in rat atria. a. Representative atrial HE staining of Day 3, Day 7, Day 11, and Day 17. The atrial myofibrils in the AF groups were more disorganized than those in the control group over time (bar = 100 μm). b. Representative atrial Masson staining of Day 3, Day 7, Day 11, and Day 17. There was no significant difference in collagen deposition between the control and AF groups (bar = 100 μm). c. The expression of collagen I in the AF groups was slightly increased from Day 13 compared with that in the control group, assessed by western blot. n = 5 in each group.

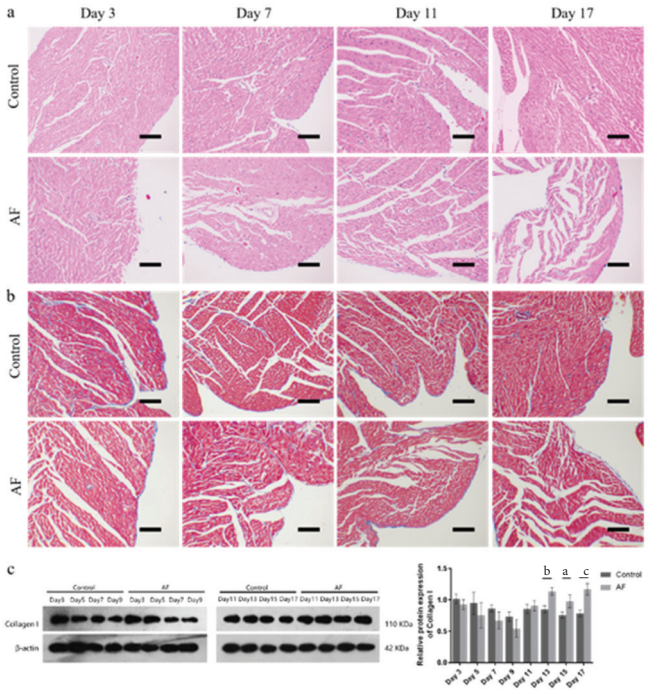

[a]$P < .05$ vs. control rats
[b]$P < .01$ vs. control rats
[c]$P < .001$ vs. control rats

Abbreviaitions: AF, atrial fibrillation; HE, hematoxylin and eosin.

RESULTS

Construction of AF rat model

The P-wave disappearance and irregular R-R intervals were observed in the AF groups after each injection of the Ach-$CaCl_2$ mixture (1 mL/Kg), indicating the successful establishment of the AF rat model (Figure 1).[17] The recorded duration time of AF after each injection is shown in Supplementary Table 2. The average duration time recorded after each injection was 13 ± 3 seconds.

Histopathological changes in the heart of AF rats

HE staining showed that myofibrils were disorganized in the atria of the AF groups compared to the control groups over time; the difference continued to expand over time even when dosing was stopped after Day 7 (Figure 2a). Masson staining showed no significant difference in collagen deposition between the control and AF groups (Figure 2b). The expression of collagen I in the AF groups was slightly increased from Day 13 compared with that in the control group ($P < .05$) (Figure 2c**,** Supplementary data 1).

The expressions of CD31 and VE-cadherin decreased, while the expressions of FSP-1 and TGF-β1 increased in the AF group (Figure 3**,** Supplementary data 1). Then, the expressions of CD31, VE-cadherin, FSP-1, and TGF-β1 were detected. Compared with the control group, the qRT-PCR result showed that the expression of CD31 in the AF group was decreased, but the difference was significant on Day 7, Day 9, and Day13; while the western blot result showed that CD31 expression decreased in the AF group, but the difference was statistically significant at Day 5, Day 11, and Day 17 (Figure 3). According to the qRT-PCR and western blot results, the expression of VE-cadherin was decreased in the AF group after Day 3 and was relatively stable after Day 9 compared with the control group (Figure 3). In contrast, the expressions of FSP-1 and TGF-β1 increased in the AF group compared with the control group (Figure 3). The expression of FSP-1 increased significantly from Day 5 to Day 9 and the difference decreased after Day 9, and the expression of TGF-β1 increased from Day 3 to Day 7 and remained stable thereafter (Figure 3).

EndMT occurred in the atria of AF rats

Two groups of immunofluorescence co-expression analyses were performed to further confirm and demonstrate the EndMT process in AF rats. In this study, EndMT was characterized by co-expression of CD31/FSP-1 or VE-cadherin/FSP-1 in ECs.[14] Co-expression of CD31/FSP-1 and VE-cadherin/FSP-1 was observed after Day 3, which only occurred in AF rat atria and was not detected in all control samples (Figure 4). In representative Day 11 atrial sections, FSP-1 was eventually co-expressed in 48.8±10.2% of CD31+ ECs and 50.2±13.2% of VE-cadherin+ ECs (Figure 4). In the endocardial layer, FSP-1+ cells comprised approximately 45% of ECs on Day 11. The coexpression of CD31/FSP-1 and VE-cadherin/FSP-1 was also found in the cardiac valvular ECs of AF rats but was not observed in the hearts of control rats (Figure 5).

Figure 3. The expressions of CD31 and VE-cadherin decreased, while the expressions of FSP-1 and TGF-β1 increased in the AF group. a-d. Relative mRNA expressions of CD31 (a), VE-cadherin (b), FSP-1 (c), and TGF-β1 (d) were assessed by qRT-PCR, GAPDH was used as a standardization control; e. The protein expressions of CD31, VE-cadherin, FSP-1, and TGF-β1 were assessed by western blot, and β-actin as control bands. n = 5 in each group.

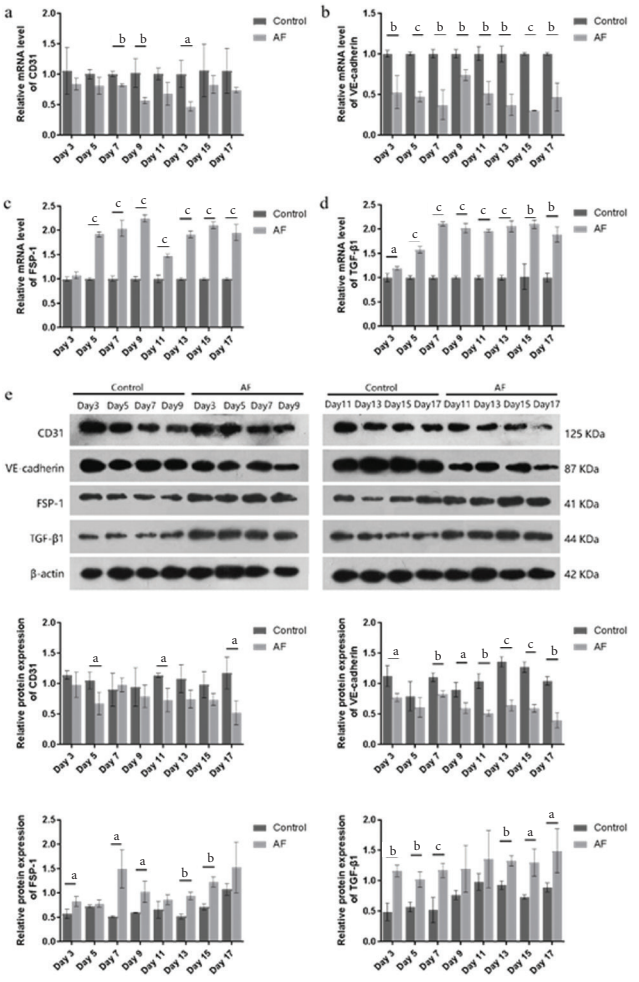

[a]$P < .05$ vs. control rats,
[b]$P < .01$ vs. control rats,
[c]$P < .001$ vs. control rats.

Note: The experiment was repeated three times, and the data were presented as mean ± standard deviation.

Abbreviaitions: AF, Atrial fibrillation; CD31, cluster of differentiation 31; VE-cadherin, vascular endothelial cadherin; FSP-1, fibroblast-specific protein-1; TGF-β1, transforming growth factor-beta 1; qRT-PCR, quantitative reverse transcription-polymerase chain reaction.

The expression of HIF-1α increased in the AF group. In addition, the expression of HIF-1α was detected in both groups. Representative atrial immunohistochemistry images showed that compared with the control group, the atrial HIF-1α (brown-colored) in AF groups increased consistently (Figure 6a). QRT-PCR and western blot showed that

Figure 4. Representative immunofluorescence images of CD31/FSP-1 and VE-cadherin/FSP-1 in rat atria. The co-expression of CD31/FSP-1 and VE-cadherin/FSP-1 was observed in the endocardial endocardium of the AF rat atria, but not in the controls (bar = 50μm).

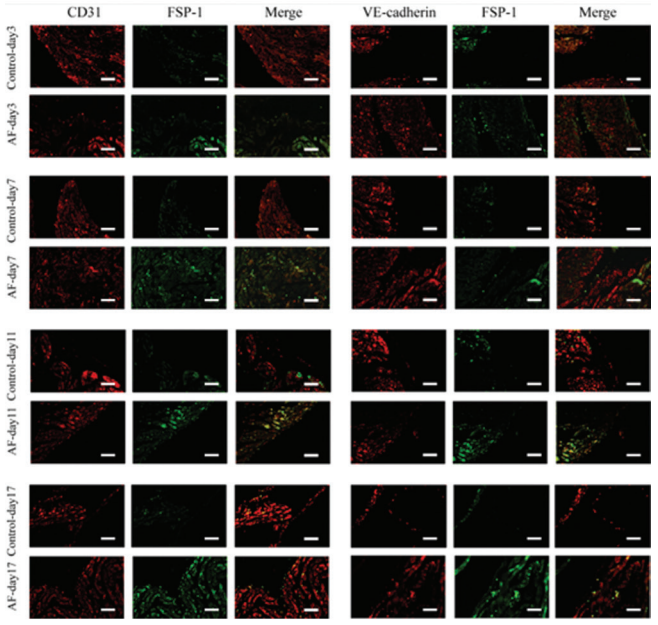

Abbreviaitions: CD31, a cluster of differentiation 31; FSP-1, fibroblast-specific protein-1; VE-cadherin, vascular endothelial cadherin; ECs, endothelial cells; AF, atrial fibrillation.

Figure 5. Representative immunofluorescence images of CD31/FSP-1 and VE-cadherin/FSP-1 in rat valves on Day 13. The co-expression of CD31/FSP-1 and VE-cadherin/FSP-1 was observed in the cardiac valvular ECs of AF rats, but not in the controls (bar = 100 μm).

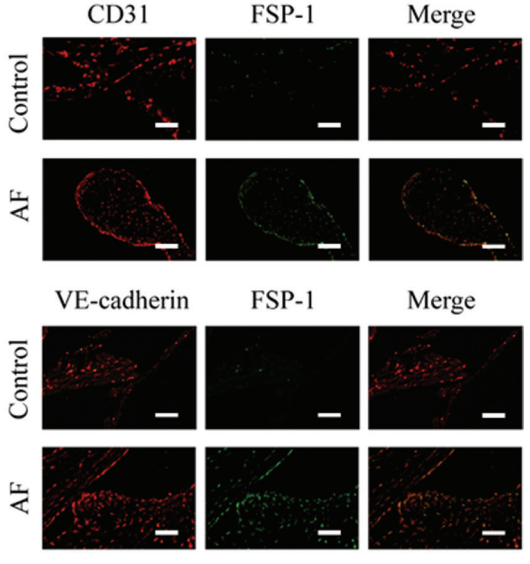

Abbreviaitions: CD31, a cluster of differentiation 31; FSP-1, fibroblast-specific protein-1; VE-cadherin, vascular endothelial cadherin; ECs, endothelial cells; AF, atrial fibrillation.

Figure 6. The expression of HIF-1α increased in AF rat atria. a. Representative atrial HIF-1α immunohistochemistry images of rat atria on Day 3, Day 7, Day 11, and Day 17, and it was found that compared with the control group, the degrees of atrial HIF-1α (brown-colored) in AF groups increased (bar = 100 μm). b-c. The protein expression of HIF-1α was assessed by western blot, and β-actin served as control bands. d. Relative mRNA expression of HIF-1α was assessed by qRT-PCR, GAPDH as a standardization control. n = 5 in all time points.

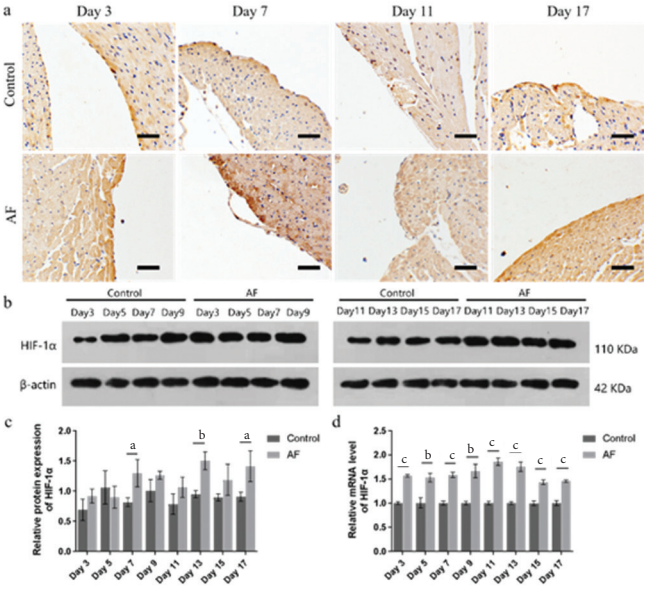

[a]$P < .05$ vs. control rats
[b]$P < .01$ vs. control rats
[c]$P < .001$ vs. control rats

Note: The experiment was repeated three times, and the data were presented as mean ± standard deviation.

Abbreviaitons: HIF-1α, hypoxia-inducible factor-1 alpha; AF, atrial fibrillation; qRT-PCR, quantitative reverse transcription-polymerase chain reaction.

compared with the control group, the expression of HIF-1α in the AF group was increased at all-time points from Day 3 (Figure 6b-d**,** Supplementary data 1).

DISCUSSION

This study demonstrated that AF could lead to EndMT in vivo. It was shown that in the AF rat model induced by daily intravenous injection of Ach-$CaCl_2$ for seven days, the EndMT process was found on Day 3 and continued until Day 17. The EndMT process was still observed after Ach-$CaCl_2$ was discontinued (Figure 4, 5). Collagen I was slightly increased in the AF groups from Day 13. Finally, we recommend Day 7-Day 17 as the optimal observation time point for this model, considering the immunofluorescence results and the expression trends of EndMT-related markers. This EndMT model of AF provides a new sight for further mechanistic discoveries and drug trials of AF.

Atrial remodeling is a crucial factor in the maintenance and progression of AF, and atrial fibrosis is the most prominent

feature of atrial remodeling.[2] EndMT-derived fibroblasts play an essential role in fibrosis, but EndMT research started late in atrial fibrosis.[4,18] Cardiac-specific TGF-β1 transgenic goats increase cardiac fibrosis and the incidence of spontaneous AF.[19] Lai et al. investigated the mechanism of EndMT in atrial fibrosis and found that endocardial ECs from the atrial appendage treated with TGF-β1 induced EndMT; in transgenic mice with cardiac-specific TGF-β1 overexpression, knockdown of miR-181b attenuated endothelial EndMT and atrial fibrosis, and reduced AF susceptibility, but the extent to which EndMT contributes to both subendocardial fibrosis and atrial fibrosis is not clear.[20] In 2016, Kato et al. first proposed that EndMT occurred in the atria of AF patients, and the level of mesenchymal markers was positively correlated with the degree of atrial structural remodeling.[11] Regretfully, the result had not been compared to normal hearts. To the best of our knowledge, there are still significant gaps in the area of the EndMT process in AF patients or animal models.

The mechanistic study of atrial fibrosis in AF has momentous clinical significance for the treatment and prognosis of AF, but few EndMT studies have been reported in AF.[11] The ECs in the heart can be divided into endocardial ECs, myocardial microvascular ECs, and coronary ECs according to location.[21] Although the location and origin are different, these ECs have abundant cellular connections, which act as a sound barrier between circulating blood and cardiomyocytes[22]; second, these ECs have high angiogenic potential and metabolic efficiency, providing sufficient oxygen and energy for the heart.[23] Excessive activation of EndMT in the heart aggravates cardiac fibrosis and affects the typical working environment of cardiomyocytes. We do not want to see it either. Therefore, we need to better understand the EndMT process in AF; the development of an appropriate EndMT model in AF can provide vital support for the study of atrial fibrosis in AF.

Typical EndMT shows definitive co-expression of mesenchymal markers in ECs, elevated FSP-1 (mesenchymal marker), and decreased expression of CD31 and VE-cadherin (endothelial cell markers).[8] We confirmed that this AF rat model had typical EndMT processes. CD31 and VE-cadherin are transmembrane glycoproteins expressed by endocardial ECs, vascular ECs, and some circulating blood cells, and they are decreased in the AF model.[24] FSP-1 was highly expressed in AF hearts, suggesting abnormal activation, proliferation, and differentiation of fibroblasts, followed by irregular synthesis and deposition of extracellular matrix (ECM) proteins, which were identified as AF substrates.[25] Current evidence from patients and animal models suggests that cardiac endothelial cells are activated through EndMT to generate a large number of cardiac fibroblasts, as a supplement to resident cardiac fibroblasts, which are involved in myocardial fibrosis and play a crucial role in cardiac remodeling.[26,27] The fibroblasts transformed from EndMT were found to be reversible and plastic by mechanistic studies[28]; therefore, the plasticity of endothelial cells can be a crucial node in preventing excessive ECM synthesis.[29]

Meanwhile, the EndMT phenomenon was observed in both endocardial ECs and vascular ECs in the AF model (Figure 4, 5). Functional valve regurgitation is common in AF patients and is often associated with atrial remodeling and annulus enlargement of mitral and tricuspid annulus.[30] Restoration of sinus rhythm can improve atrial remodeling and valve regurgitation.[31] The findings of this study provide an alternative hypothesis: AF affects the pathophysiological changes of the valve itself, reducing valve compliance and increasing the probability of valve regurgitation. This needs further research to be verified.

Additionally, the levels of TGF-β1 and HIF-1α were both increased in the early stage of AF (Day 3-Day 17) (vs. the control group at the same time point). TGF-β1 induces EndMT in cells, promoting the expression of transcription factors such as FSP-1, Snail and et. al.[32] These have been described as significant regulators of EndMT.[33] ECs have a unique transcriptional response program to TGF-β in the early stages after injury, with an EndMT process of adaptive phenotypic change.[34] This adaptive phenotypic change is reversible.[28] Hypoxia-induced neovascularization is partially mediated by clonal amplification of ECs, which show enrichment of EndMT-related genes, suggesting that hypoxia-enhanced EndMT may contribute to vascular growth under ischemia.[35] The resilient changes of ECs in response to acute stress may help the body to adapt to the injury and contribute to repair and regeneration, which is important for the prevention of chronic dysfunction significance.[35,36]

The elevated levels of HIF-1α supported that the hearts in AF rats were undergoing a persistent hypoxic state, and it should be noted that the elevation of HIF-1α after AF occurred earlier than TGF-β1.[37] Previous studies showed that HIF-1α can activate the TGF-β/Smad pathway, which inhibits cell apoptosis and promotes the proliferation of fibroblasts under tissue hypoxia.[38] On the basis that TGF-β1 is a well-recognized driver of EndMT, HIF-1α may be another driver or participant of EndMT in AF progression. This study first provided insight into the potential link between HIF-1α and EndMT in AF.

Limitations

The limitation of this study is that we could not reproduce and verify all AF animal models; after all, there are many species and modeling methods of AF.[39] Therefore, in this pilot study, we selected a common small experimental animal, the SD rat, as the carrier for AF modeling and experiments. A previous study found that the EndMT activity and expression of TGF-β1 in the left ventricle were increased in a canine model of right ventricular pacing-induced heart failure, leading to aggravation of cardiac fibrosis in the left ventricle.[9] Therefore, intravenous drug injection (Ach-$CaCl_2$) was selected to induce non-sustained AF, to rule out the possible atrial EndMT caused by rapid right atrial pacing and focus on the objective of abnormal electrical activity.[39] Other modeling methods will be tested in a follow-up study.

CONCLUSION

In conclusion, this study confirmed that the EndMT process appeared in the ultra-early stage of the AF rat atria and was the first study to explore the dynamic process of EndMT in an AF model. It provided an economical and applicable animal model to study the EndMT process in AF for most researchers. Furthermore, the expression of HIF-1α increased in AF rat atria. It has been reported that HIF-1α is associated with the regulation of the EndMT process. Then HIF-1α may be similarly involved in EndMT during AF. This study provides a theoretical basis and experimental methods for the prevention, detection, and early intervention of cardiac remodeling in AF, as well as the discovery of new targets for reversing cardiac remodeling.

ACKNOWLEDGMENT

None.

FUNDINGS

This research was supported by the Key Discipline Cluster of Pudong New Area Health Committee (Grant No. PWZxq2022-11), the Peak Discipline Construction of Pudong New Area Health Committee (Grant No. PWYgf2021-04), and the Epidemiological Investigation of Atrial Fibrillation in Pudong New Area and Prospective Cohort Study on Whole-process Management of A+trial Fibrillation under Hierarchical Diagnosis and Treatment Mode (Grant No. PKJ2021-Y33).

DATA AVAILABILITY

The experimental data used to support the findings of this study are available from the corresponding author upon request.

CONFLICT OF INTEREST

The authors declare that there is no conflict of interest.

REFERENCES

1. Chung MK, Refaat M, Shen WK, et al; ACC Electrophysiology Section Leadership Council. Atrial Fibrillation: JACC Council Perspectives. *J Am Coll Cardiol*. 2020;75(14):1689-1713. doi:10.1016/j.jacc.2020.02.025
2. Li CY, Zhang JR, Hu WN, Li SN. Atrial fibrosis underlying atrial fibrillation (Review). [Review]. *Int J Mol Med*. 2021;47(3):9. doi:10.3892/ijmm.2020.4842
3. Tallquist MD, Molkentin JD. Redefining the identity of cardiac fibroblasts. *Nat Rev Cardiol*. 2017;14(8):484-491. doi:10.1038/nrcardio.2017.57
4. Stenmark KR, Frid M, Perros F. Endothelial-to-Mesenchymal Transition. *Circulation*. 2016;133(18):1734-1737. doi:10.1161/CIRCULATIONAHA.116.022479
5. Alonso-Herranz L, Sahún-Español Á, Paredes A, et al. Macrophages promote endothelial-to-mesenchymal transition via MT1-MMP/TGFβ1 after myocardial infarction. *eLife*. 2020;9:e57920. doi:10.7554/eLife.57920
6. Wang M, Liu Y, Dai L, et al. ONX0914 Inhibition of Immunoproteasome Subunit LMP7 Ameliorates Diabetic Cardiomyopathy via Restraining endothelial-mesenchymal Transition. *Clinical Science (London, England: 1979)*. 2023;137(16):1297-1309. doi:10.1042/CS20230732
7. Wilhelmi T, Xu X, Tan X, et al. Serelaxin alleviates cardiac fibrosis through inhibiting endothelial-to-mesenchymal transition via RXFP1. *Theranostics*. 2020;10(9):3905-3924. doi:10.7150/thno.38640
8. Zhang L, He J, Wang J, et al. Knockout RAGE alleviates cardiac fibrosis through repressing endothelial-to-mesenchymal transition (EndMT) mediated by autophagy. *Cell Death Dis*. 2021;12(5):470. doi:10.1038/s41419-021-03750-4
9. Mai J, Hu Q, Xie Y, et al. Dyssynchronous pacing triggers endothelial-mesenchymal transition through heterogeneity of mechanical stretch in a canine model. *Circ J*. 2015;79(1):201-209. doi:10.1253/circj.CJ-14-0721
10. Zhang S, Li Y, Huang X, et al. Seamless Genetic Recording of Transiently Activated Mesenchymal Gene Expression in Endothelial Cells During Cardiac Fibrosis. *Circulation*. 2021;144(25):2004-2020. doi:10.1161/CIRCULATIONAHA.121.055417
11. Kato T, Sekiguchi A, Sagara K, et al. Endothelial-mesenchymal transition in human atrial fibrillation. *J Cardiol*. 2017;69(5):706-711. doi:10.1016/j.jjcc.2016.10.014
12. National Research Council (US) Committee for the Update of the Guide for the Care and Use of Laboratory Animals. *Guide for the Care and Use of Laboratory Animals*. 8th ed. National Academies Press (US); 2011. https://pubmed.ncbi.nlm.nih.gov/21595115/
13. Zhu J, Zhu N, Xu J. miR101a3p overexpression prevents acetylcholineCaCl$_2$induced atrial fibrillation in rats via reduction of atrial tissue fibrosis, involving inhibition of EZH2. *Mol Med Rep*. 2021;24(4):740. doi:10.3892/mmr.2021.12380
14. Xie Y, Liao J, Yu Y, et al. Endothelialtomesenchymal transition in human idiopathic dilated cardiomyopathy. *Mol Med Rep*. 2018;17(1):961-969. doi:10.3892/mmr.2017.8013
15. Zou D, Geng N, Chen Y, et al. Ranolazine improves oxidative stress and mitochondrial function in the atrium of acetylcholine-CaCl2 induced atrial fibrillation rats. *Life Sci*. 2016;156:7-14. doi:10.1016/j.lfs.2016.05.026
16. Zhang W, Yuan W, Song J, Wang S, Gu X. LncRNA CPS1-IT1 suppresses EMT and metastasis of colorectal cancer by inhibiting hypoxia-induced autophagy through inactivation of HIF-1α. *Biochimie*. 2018;144:21-27. doi:10.1016/j.biochi.2017.10.002
17. Lv X, Li J, Hu Y, et al. Overexpression of miR-27b-3p Targeting Wnt3a Regulates the Signaling Pathway of Wnt/β-Catenin and Attenuates Atrial Fibrosis in Rats with Atrial Fibrillation. *Oxid Med Cell Longev*. 2019;2019:5703764. doi:10.1155/2019/5703764
18. Zeisberg EM, Tarnavski O, Zeisberg M, et al. Endothelial-to-mesenchymal transition contributes to cardiac fibrosis. *Nat Med*. 2007;13(8):952-961. doi:10.1038/nm1613
19. Regouski M, Galenko O, Doleac J, et al. Spontaneous Atrial Fibrillation in Transgenic Goats With TGF (Transforming Growth Factor)-β1 Induced Atrial Myopathy With Endurance Exercise. *Circ Arrhythm Electrophysiol*. 2019;12(11):e007499. doi:10.1161/CIRCEP.119.007499
20. Lai YJ, Tsai FC, Chang GJ, et al. miR-181b targets semaphorin 3A to mediate TGF-β-induced endothelial-mesenchymal transition related to atrial fibrillation. *J Clin Invest*. 2022;132(13):e142548. doi:10.1172/JCI142548
21. Zou X, Song XM, Wang J. [Biological features of cardiac endothelial cells and their role and mechanism on regulating heart failure]. *Zhonghua Xin Xue Guan Bing Za Zhi*. 2021;49(4):318-323. doi:10.3760/cma.j.cn112148-20200521-00418
22. Marcu R, Choi YJ, Xue J, et al. Human Organ-Specific Endothelial Cell Heterogeneity. *iScience*. 2018;4:20-35. doi:10.1016/j.isci.2018.05.003
23. Alexander Y, Osto E, Schmidt-Trucksäss A, et al. Endothelial function in cardiovascular medicine: a consensus paper of the European Society of Cardiology Working Groups on Atherosclerosis and Vascular Biology, Aorta and Peripheral Vascular Diseases, Coronary Pathophysiology and Microcirculation, and Thrombosis. *Cardiovasc Res*. 2021;117(1):29-42. doi:10.1093/cvr/cvaa085
24. Muller WA. Localized signals that regulate transendothelial migration. *Curr Opin Immunol*. 2016;38:24-29. doi:10.1016/j.coi.2015.10.006
25. Reese-Petersen AL, Olesen MS, Karsdal MA, Svendsen JH, Genovese F. Atrial fibrillation and cardiac fibrosis: A review on the potential of extracellular matrix proteins as biomarkers. *Matrix Biol*. 2020;91-92:188-203. doi:10.1016/j.matbio.2020.03.005
26. Liu ZH, Zhang Y, Wang X, et al. SIRT1 activation attenuates cardiac fibrosis by endothelial-to-mesenchymal transition. *Biomed Pharmacother*. 2019;118:109227. doi:10.1016/j.biopha.2019.109227
27. Xu L, Fu M, Chen D, et al. Endothelial-specific deletion of Ets-1 attenuates Angiotensin II-induced cardiac fibrosis via suppression of endothelial-to-mesenchymal transition. *BMB Rep*. 2019;52(10):595-600. doi:10.5483/BMBRep.2019.52.10.206
28. Fang JS, Hultgren NW, Hughes CCW. Regulation of Partial and Reversible Endothelial-to-Mesenchymal Transition in Angiogenesis. *Front Cell Dev Biol*. 2021;9:702021. doi:10.3389/fcell.2021.702021
29. Dejana E, Hirschi KK, Simons M. The molecular basis of endothelial cell plasticity. *Nat Commun*. 2017;8(1):14361. doi:10.1038/ncomms14361
30. Ortiz-Leon XA, Posada-Martinez EL, Trejo-Paredes MC, et al. Tricuspid and mitral remodelling in atrial fibrillation: a three-dimensional echocardiographic study. *Eur Heart J Cardiovasc Imaging*. 2022;23(7):944-955. doi:10.1093/ehjci/jeac045
31. Soulat-Dufour L, Lang S, Addetia K, et al. Restoring Sinus Rhythm Reverses Cardiac Remodeling and Reduces Valvular Regurgitation in Patients With Atrial Fibrillation. *J Am Coll Cardiol*. 2022;79(10):951-961. doi:10.1016/j.jacc.2021.12.029
32. Song S, Liu L, Yu Y, et al. Inhibition of BRD4 attenuates transverse aortic constriction- and TGF-β-induced endothelial-mesenchymal transition and cardiac fibrosis. *J Mol Cell Cardiol*. 2019;127:83-96. doi:10.1016/j.yjmcc.2018.12.002
33. Hata A, Chen YG. TGF-β Signaling from Receptors to Smads. *Cold Spring Harb Perspect Biol*. 2016;8(9):a022061. doi:10.1101/cshperspect.a022061
34. Tombor LS, John D, Glaser SF, et al. Single cell sequencing reveals endothelial plasticity with transient mesenchymal activation after myocardial infarction. *Nat Commun*. 2021;12(1):681. doi:10.1038/s41467-021-20905-1
35. Manavski Y, Lucas T, Glaser SF, et al. Clonal Expansion of Endothelial Cells Contributes to Ischemia-Induced Neovascularization. *Circ Res*. 2018;122(5):670-677. doi:10.1161/CIRCRESAHA.117.312310
36. Tombor LS, Dimmeler S. Why is endothelial resilience key to maintain cardiac health? *Basic Res Cardiol*. 2022;117(1):35. doi:10.1007/s00395-022-00941-8
37. Babapoor-Farrokhran S, Gill D, Alzubi J, Mainigi SK. Atrial fibrillation: the role of hypoxia-inducible factor-1-regulated cytokines. *Mol Cell Biochem*. 2021;476(6):2283-2293. doi:10.1007/s11010-021-04082-9
38. Lei R, Li J, Liu F, et al. HIF-1α promotes the keloid development through the activation of TGF-β/Smad and TLR4/MyD88/NF-κB pathways. *Cell Cycle*. 2019;18(23):3239-3250. doi:10.1080/15384101.2019.1670508
39. Schüttler D, Bapat A, Kääb S, et al. Animal Models of Atrial Fibrillation. *Circ Res*. 2020;127(1):91-110. doi:10.1161/CIRCRESAHA.120.316366

Supplementary Table 1. The primer sequences

Name	5'-3'
HIF-1α	F: TCTCCATCTCCTACCCACATACA
	R: TGCTCTGTTTGGTGAGGCTGT
CD31	F: GGTAATAGCCCCGGTGGATG
	R: TTCTTCGTGGAAGGGTCTGC
FSP-1	F: ACCTCTCTGTTCAGCACTTCC
	R: GAACTTGTCACCCTCGTTGC
TGF-β1	F: GTGGCTGAACCAAGGAGACGGAATA
	R: ACCTCGACGTTTGGGACTGATC
VE-cadherin	F: AATTTGCCCAGCCCTACGAACCTA
	R: TGCTCCCGATTAAACTGTC CATAC
GAPDH	F: GCAACTAGGATGGTGTGGCT
	R: TCCCATTCCCCAGCTCTCATA

Abbreviations: HIF-1α, hypoxia-inducible factor-1 alpha; CD31, cluster of differentiation 31; FSP-1, fibroblast-specific protein-1; TGF-β1, transforming growth factor-beta 1; VE-cadherin, vascular endothelial cadherin; GAPDH, glyceraldehyde phosphate dehydrogenase.

Supplementary Table 2. The duration time of AF recorded in the AF group from Day 1 to Day 7

Time	AF Group (n = 5)
Day 1 (s)	9±1
Day 2 (s)	10±1
Day 3 (s)	12±2
Day 4 (s)	12±3
Day 5 (s)	14±3
Day 6 (s)	15±4
Day 7 (s)	16±3

Abbreviations: AF, Atrial fibrillation; s, seconds.